THE ROYAL SOCIETY

The thermochemical structure and evolution of Earth's mantle: constraints and numerical models

By Paul J. Tackley and Shunxing Xie

Department of Earth and Space Sciences and Institute of Geophysics and Planetary Physics, University of California, Los Angeles, 595 Charles Young Drive East, Los Angeles, CA 90095-1567, USA (ptackley@ucla.edu)

Geochemical observations place several constraints on geophysical processes in the mantle, including a requirement to maintain several distinct reservoirs. Geophysical constraints limit plausible physical locations of these reservoirs to a thin basal layer, isolated deep 'piles' of material under large-scale mantle upwellings, high-viscosity blobs/plums or thin strips throughout the mantle, or some combination of these. A numerical model capable of simulating the thermochemical evolution of the mantle is introduced. Preliminary simulations are more differentiated than Earth but display some of the proposed thermochemical processes, including the generation of a high-μ mantle reservoir by recycling of crust, and the generation of a high-^{3}He/^{4}He reservoir by recycling of residuum, although the resulting high-^{3}He/^{4}He material tends to aggregate near the top, where mid-ocean-ridge melting should sample it. If primitive material exists as a dense basal layer, it must be much denser than subducted crust in order to retain its primitive (e.g. high-^{3}He) signature. Much progress is expected in the near future.

Keywords: mantle convection; plate tectonics; geochemistry; chemical evolution

1. Introduction

From geochemical observations it is clear that the mantle is chemically heterogeneous (e.g. Hofmann 1997). Geochemical observations offer important constraints on the structure and evolution of the mantle yet, despite some pioneering efforts, have typically been under-considered by the geophysical community. Indeed, geophysical models of mantle structure have often been inconsistent with geochemical constraints, while geochemical mantle models have been inconsistent with geophysical constraints (Tackley 2000a).

The physical evolution and chemical evolution of the plate–mantle system are inextricably coupled. The plate–mantle system influences chemical evolution through the complementary processes of differentiation (caused by melting) and mixing (of, for example, subducted/recycled or primordial components). Conversely, compositional

variations influence the plate–mantle system through the effect of composition on buoyancy, viscosity (e.g. presence of water) and 'strength' in general, and the effect of radiogenic heating.

We are now at the point where it is becoming possible to combine models of mantle geochemical evolution with geophysical models of mantle and plate dynamics, in order to test hypotheses regarding mantle thermochemical structure and dynamics, and hence to constrain the range of feasible models. This paper begins by briefly reviewing geochemical constraints on mantle structure and discussing relevant constraints from geophysical modelling and observations. An integrated model of mantle major- and trace-element evolution, convection and plate tectonics is then introduced and preliminary simulation results are presented. Finally, plausible models are outlined, together with directions for future investigation.

2. Constraints from geochemistry

(a) General

The implications of geochemical observations for constraining mantle structure and dynamics are briefly reviewed. Of key importance is the inferred existence of several reservoirs, the physical location of which must be explained.

(i) Isotopic heterogeneities and length-scales

The relative homogeneity of mid-ocean-ridge basalts (MORBs) and heterogeneity of ocean-island basalts (OIBs) implies that substantial isotopic heterogeneity exists at short length-scales: the sampling region is presumed to be larger in the case of MORBs (Allègre & Turcotte 1986). However, although OIB compositions overlap MORBs, it seems clear that the isotopic composition of MORBs is not simply the averaged isotopic composition of OIB, implying that OIBs involve some mixing from other reservoirs (see below) (Hofmann 1997).

(ii) Outgassed fraction of the mantle

The fraction of the mantle that has been processed through mid-ocean-ridge or other melting environments is constrained by the amount of radiogenic argon (^{40}Ar) in the atmosphere combined with an estimate of the amount of ^{40}K in the solid Earth. This suggests that *ca.* 50% of the mantle has outgassed (Allègre *et al.* 1996), although this figure is rather uncertain, mainly because the amount of ^{40}K in the mantle is uncertain, with K/U estimates ranging from 2800 (Stacey 1992) to 20 000. Low concentrations of Ar are inferred in the MORB source, suggesting the existence of a deeper, undegassed reservoir in order to account for the expected amount of ^{40}Ar in the mantle, although this difficulty could be resolved if the amount of ^{40}K were lower than commonly estimated (Albarède 1998; Davies 1999).

(iii) Lateral mixing

This is constrained by the requirement to maintain distinctly different isotopic domains, notably the DUPAL anomaly (Castillo 1988; Hart 1984).

(b) Reservoirs

Several reservoirs have been identified, based either on trace-element ratios in MORBs and OIBs or on cosmochemical arguments.

Recycled. The high-μ mantle (HIMU) and enriched mantles' (EM1, EM2) end-members are identified from trace-element ratios of MORB and OIBs (Hofmann 1997). HIMU is often identified as subducted oceanic crust, and EM1 and EM2 as recycled continental material. The slope of the MORB-to-OIB trend on lead-isotope diagrams gives a mean age of 1–2 Gyr, although this 'age' is not straightforwardly interpretable (Albarède 2001; Hofmann 1997).

High ^{3}He/^{4}He. Whereas the ^{3}He/^{4}He ratio in MORB displays a narrow range of values around eight times the atmospheric ratio, OIBs display a much wider scatter, with some (e.g. Loihi) having values up to 30 times the atmospheric ratio. This reservoir has generally been assumed to be primordial and outgassed, because ^{3}He is primordial, whereas ^{4}He is produced by radioactive decay of U and Th. However, it has recently been argued that high-^{3}He/^{4}He could be caused by recycled depleted lithosphere (Coltice *et al.* 2000; Coltice & Ricard 1999; Ferrachat & Ricard 2001). Although it was previously thought that this requires He to be less incompatible than U and Th (e.g. Graham *et al.* 1990), so that He ratios are frozen in the residuum at the time of melting, the above authors showed that this is not necessary if residuum can be stored for substantial time periods while the rest of the mantle becomes substantially outgassed.

Mass balance. There is argued to be a primitive, primordial reservoir containing 'missing' trace elements, including heat-producing elements (HPEs) and ^{40}Ar. This argument is based on subtracting a model of continental composition and a model of depleted MORB mantle composition from a model of bulk-silicate-Earth composition: a significant fraction of the expected abundance of several elements is 'missing'. This is consistent with the low concentrations of HPEs in the MORB source, which are insufficient to explain the Earth's heat flow, implying that there must be some HPEs concentrated elsewhere. This reservoir may make up 10–50% of the Earth's mantle and is also 'hidden', in the sense that it produces no geochemical (and, apparently, no geophysical) signature. It is difficult for it to also simultaneously be the high-^{3}He/^{4}He reservoir because it is enriched in U and Th, which produce large amounts of ^{4}He by radioactive decay.

3. Constraints from geophysical studies

(a) Mixing

(i) *Two-dimensional mixing*

Two-dimensional simulations of simple mantle convection (Christensen 1989; Kellogg & Turcotte 1990; Schmalzl & Hansen 1994) suggest that for whole-mantle convection the mantle should be homogenized in a time-scale of less than 1 Gyr, although unmixed islands may remain. Non-Newtonian rheology, which is thought to be important in the upper mantle (Karato & Wu 1993), may somewhat inhibit mixing (Ten *et al.* 1998). The rate at which blobs of anomalous (e.g. primitive) material are stretched

and assimilated into the flow depends on their relative viscosity; very viscous blobs can survive intact for many mantle overturns (Manga 1996).

(ii) *Three-dimensional mixing*

In three-dimensional geometry with only poloidal flow, mixing may be significantly less efficient than in two dimensions (Schmalzl *et al.* 1995, 1996) but, if the toroidal flow associated with plate motions is included (Gable *et al.* 1991), mixing can instead be more efficient (Ferrachat & Ricard 1998).

(iii) *Deep-mantle mixing*

High viscosity in the deep mantle is not sufficient to maintain different reservoirs over geological time-scales (Ferrachat & Ricard 2001; van Keken & Ballentine 1998, 1999), in contrast to predictions from earlier calculations at lower convective vigour (Gurnis & Davies 1986). Part of the reason for this apparent discrepancy is that the latter study used a kinematically driven flow rather than buoyancy-driven flow. Since a viscosity jump does not affect densities, thermal buoyancy-driven flow has no problem crossing it, so substantial mass exchange occurs between upper and lower mantles. Buoyancy is thus necessary to maintain separate reservoirs.

(*b*) *Layering and outgassing*

(i) *Outgassing*

The observed total amount of ^{40}Ar outgassing is consistent with whole-mantle convection (van Keken & Ballentine 1998, 1999); mantle layering is not required. More problematic is the very low concentration of ^{40}Ar observed in the MORB source, which seems to require concentration of the remaining ^{40}Ar in a deeper layer (e.g. Allègre *et al.* 1996). However, if the amount of ^{40}K were lower than commonly estimated, this difficulty could be overcome (Albarède 1998; Davies 1999).

(ii) *Layering at* 660 km

The mantle is not completely layered at the 660 km discontinuity, although the descent of slabs may often be temporarily interrupted at that depth. We know this because seismic tomographic models of increasing resolution and quality (e.g. Masters *et al.* 2000; van der Hilst *et al.* 1997) show that slabs are observed to penetrate the lower mantle, and because the 660 km discontinuity is now known to correspond to the spinel-to-perovskite-plus-magnesiowüstite phase transition, which simulations indicate is unable to completely layer the convection, although local and intermittent layering is possible (Brunet & Machetel 1998; Butler & Peltier 1997; Christensen 1996; Tackley 1996*b*; Tackley *et al.* 1994).

(iii) *Thick, deep layer?*

A very deep (e.g. *ca.* 1000 km) stable layer, as proposed by Kellogg *et al.* (1999), generates very-high-amplitude heterogeneity in the mid-lower mantle, which is inconsistent with seismic tomographic models (Tackley 2002). This is true even if the contributions of temperature and composition to seismic velocity cancel out. In addition,

such a deep layer would become excessively hot (McNamara & van Keken 2000), possibly causing partial melting and making it difficult for sufficient heat to leave the core to drive the geodynamo. Most seismic tomographic models (e.g. Grand *et al.* 1997; Masters *et al.* 2000) suggest that slabs reach the core–mantle boundary (CMB) in many areas. The boundary of such a layer has not been detected by any seismic means (Vidale *et al.* 2001). Thus, the geophysical evidence weighs against the existence of a global, thick, deep layer.

(iv) *Thin or intermittent deep layer*

Several lines of evidence argue in favour of a thin (*ca.* 200–300 km thick) and/or intermittently thick deep layer. The strong seismic heterogeneity in D'' (Jeanloz & Lay 1993; Lay *et al.* 1998) and the discontinuity above this (Lay & Helmberger 1983) have long been interpreted in terms of chemically distinct material, although alternative explanations exist (Sidorin *et al.* 1999). Dense material near the CMB is swept into 'piles' underneath upwellings (Tackley 1998) and thinned, possibly to zero, under downwellings. Such dense 'piles' may be embedded in the two seismically observed 'megaplumes' under the Pacific and Africa. These megaplumes are sharp sided (Ritsema *et al.* 1998) and buoyant near the top, but could be dense deeper down (Gurnis *et al.* 2000; Ishii & Tromp 1999), as is expected for stable structures. Isolated dense piles are consistent with the heterogeneity structure of seismic tomographic models (Tackley 2002). Numerical calculations have demonstrated the dynamical feasibility of forming a layer of subducted oceanic crust at the base of the mantle with a HIMU signature (Christensen & Hofmann 1994).

(*c*) *Where could the reservoirs be?*

From the above constraints, long-lived reservoirs in the mantle must be either dense, forming a basal layer, or highly viscous, advected everywhere but resisting stretching and mixing. The following are considered plausible locations for geochemical reservoirs in the mantle.

(i) A layer that is swept into isolated 'piles', probably contained within the seismically observed 'megaplumes'. Numerical simulations (Tackley 1998) demonstrate the possible form that these would take. This could apply to either primitive or recycled crustal material, or some mixture.

(ii) A thin, laterally variable dense layer, related to the seismically observed D''. Various numerical and laboratory models have studied the form of such a layer (e.g. Montague *et al.* 1998; Olson & Kincaid 1991).

(iii) Neutrally buoyant material wafting around in the mantle. This could either be in the form of 'blobs' or 'plums' (Becker *et al.* 1999; Davies 1984) which resist stretching due to high viscosity (Manga 1996), or as thin strips, stretched by convective motions, as in the 'marble cake' model (Allègre & Turcotte 1986; Phipps Morgan & Morgan 1999). It is conceivable that the blobs could preferentially exist in the lower mantle (Becker *et al.* 1999) if they are denser than regular mantle, due to the chemical filter effect (Weinstein 1992).

4. Modelling mantle thermochemical evolution

Here, a new model is introduced that integrates geochemical tracking, mantle convection and self-consistently generated plate tectonics. This is an improvement on previous convection models with geochemical tracking both in the range of elements tracked and in the physical realism: previous models used prescribed plate motions (Christensen & Hofmann 1994) or composition that did not affect buoyancy (Ferrachat & Ricard 2001). The present model has been developed as a tool for testing hypotheses about the Earth's thermochemical evolution. Some preliminary results are presented. The model has been developed by adding tracking of trace- and major-element evolution to a well-established mantle-convection code named STAG3D (e.g. Tackley 1993). The physical model is described thoroughly elsewhere (Tackley 1996*a*, 1998, 2002) so is only briefly summarized here, but the chemical model is described in detail. The treatment of chemical species has many similarities to the treatment used in Christensen & Hofmann (1994).

(*a*) *Physics*

(i) *Thermodynamics*

The compressible anelastic approximation is assumed in two-dimensional cylindrical geometry, with depth-dependent physical properties (density, thermal diffusion, thermal expansivity) based on mineral physics results (e.g. Chopelas & Boehler 1992; Hofmeister 1999). The form of depth-dependent properties is as in Tackley (2002). The parameters are intended to be Earth like, with the exception of viscosity, which is too high, resulting in a surface Rayleigh number (defined using the reference upper mantle viscosity) of 2.0×10^6. The main effect of such depth-dependent properties is to reduce the vigour of convection and increase the size of convective features in the deep mantle (Tackley 2002).

(ii) *Rheology and plate tectonics*

Viscosity varies by six orders of magnitude with temperature, and one order of magnitude (exponentially) with depth. A pseudoplastic yield stress is included to prevent the formation of the rigid lid that would normally occur with strong temperature dependence of viscosity. This gives a self-consistent approximation of plate-like behaviour (e.g. Moresi & Solomatov 1998; Tackley 2000*b*, *c*), with essentially rigid plates separated by passive spreading centres and 'subduction zones' that form and evolve naturally with the convection. However, the obtained 'subduction zones' are double-sided (symmetric) and therefore only a crude approximation of the single-sided subduction on Earth. By setting the yield stress to high values, the model can also be used to study the thermochemical evolution of rigid-lid planets such as Mars or Venus, or planets with hypothesized episodic plate tectonics (Turcotte 1993).

(*b*) *Chemistry*

(i) *Major elements*

For initial simulations a simple two-component major element model is assumed, in which the composition ranges from 'crust' (i.e. basalt/eclogite) to 'residuum'

Table 1. *Partition coefficients and initial concentrations*

isotope	D	initial conc. (atoms g^{-1})
^{3}He	0.07	5.4×10^{10}
^{4}He	0.07	5.28×10^{14}
^{36}Ar	0.05	1.26×10^{16}
^{40}Ar	0.05	1.82×10^{18}
^{40}K	0.01	2.46×10^{19}
^{147}Sm	0.1	1.41×10^{12}
^{238}U	0.007	8.18×10^{13}
^{235}U	0.007	1.19×10^{13}
^{204}Pb	0.07	6.15×10^{12}
^{206}Pb	0.07	7.77×10^{13}
^{207}Pb	0.07	8.24×10^{13}
^{232}Th	0.007	2.18×10^{14}
^{143}Nd	0.07	3.16×10^{12}
^{144}Nd	0.07	6.14×10^{12}

(i.e. harzburgite). While this should be adequate to model oceanic plates, a major limitation of the model is that continental crust, which probably requires water migration from the subducting slab, cannot form. The mantle is initially assumed to consist of 25% eclogite and 75% harzburgite, which self-consistently differentiate as described below. It is important to note that in this model the thickness of the crust and the thickness and composition (i.e. degree of depletion) of the depleted layer arise self-consistently, rather than being assumed, as in some previous models (e.g. Christensen & Hofmann 1994; Ferrachat & Ricard 2001). In the presented cases, density is assumed to vary linearly with composition between the end-members of basalt/eclogite and harzburgite, with a total density variation of 2.5% of the surface density, or 82 kg m^{-3}, the eclogite end-member being denser except in the shallowest 60 km, where basalt is less dense. This density variation is lower than realistic for the upper mantle and top of the lower mantle (e.g. Ringwood 1990), but considerable uncertainty exists in the deep mantle, where 'eclogite' may even become less dense than pyrolite (Kesson *et al.* 1998; Ono *et al.* 2001).

(ii) *Minor elements*

The present model tracks ^{207}Pb, ^{206}Pb, ^{204}Pb, ^{235}U, ^{238}U, ^{3}He, ^{4}He ^{36}Ar, ^{40}Ar, ^{40}K, ^{232}Th, ^{143}Nd, ^{144}Nd and ^{147}Sm (although the latter three are not presented here), including relevant radioactive-decay chains. Local heating rates depend on the local concentration of heat-producing elements.

(iii) *Melting and fractionation*

Melting is calculated in each grid cell at each time-step, i.e. incremental batch melting, and melt is immediately erupted to form a surface crust. Melt is generated in a cell when the cell's temperature exceeds a depth (pressure) and composition-dependent solidus based on experimental data (Herzberg *et al.* 2000; Zerr *et al.* 1998).

The melt fraction generated during a melting event is that required to bring the temperature back onto the solidus. Only the basaltic component can melt; once the composition reaches 'harzburgite', further melting is not permitted. The assumption of immediate melt eruption physically means that melt percolation and eruption happen on a short time-scale compared with the numerical time-step. Melt is placed at the surface as 'crust' and the remaining material vertically compacts accordingly. In each melting event, trace-elements partition between the melt and the residuum (conserving mass) with partition coefficients (table 1) taken from Hiyagon & Ozima (1986) for noble gases and Christensen & Hofmann (1994) and Hofmann (1988) for other elements. For the models presented here it is assumed that noble gases entering the melt are 99% released to the atmosphere (outgassed) on eruption/crustal formation.

(iv) *Initial condition*

Because the current model does not allow for the formation of continental crust, the initial trace-element composition is based on a model of mantle composition after continental crust extraction (Christensen & Hofmann 1994; Hofmann 1988). Two initial conditions are considered here. In case H the mantle is initially homogeneous. In case L the mantle initially includes a 'primitive' dense layer with a thickness of 20% of the mantle depth (i.e. 578 km) that is enriched in trace elements and in ^{3}He. The initial concentrations of most elements are modified from those in table 1 by assuming that 50% of trace elements reside in this layer, with the other 50% residing in the rest of the mantle. The initial concentration of ^{3}He is calculated so that the present-day value of ^{3}He/^{4}He would be eight times the atmospheric value in the upper layer and 35 times the atmospheric value in the lower layer, if no differentiation or mixing occurred.

(*c*) *Numerics*

A version of the well-established finite-volume/difference multi-grid code STAG3D (Tackley 1993, 1998, 2002) is used, with the addition of tracer-particle-based trace-element tracking and crustal production. Two types of tracer particles are defined, one representing 'crust' and one 'residuum', and all tracers carry the full range of trace elements. For each time-step the amount of melting in each cell is calculated and trace elements are redistributed (fractionated) between the (basalt) tracers that melt and the tracers that do not melt. Melted tracers are then placed at the top of the system and compaction is accounted for.

5. Simulation results

(*a*) *Cases and realism*

Although several cases have so far been run, this paper focuses on two, the only difference being the initial condition (homogeneous or layered). The models presented are short of being Earth like in several respects, the most important of which are convective vigour and viscosity/rheology; limitations that are for the moment imposed by the numerical solver and the computer resources available. However, the results illustrate several processes that have been proposed to occur in Earth and are
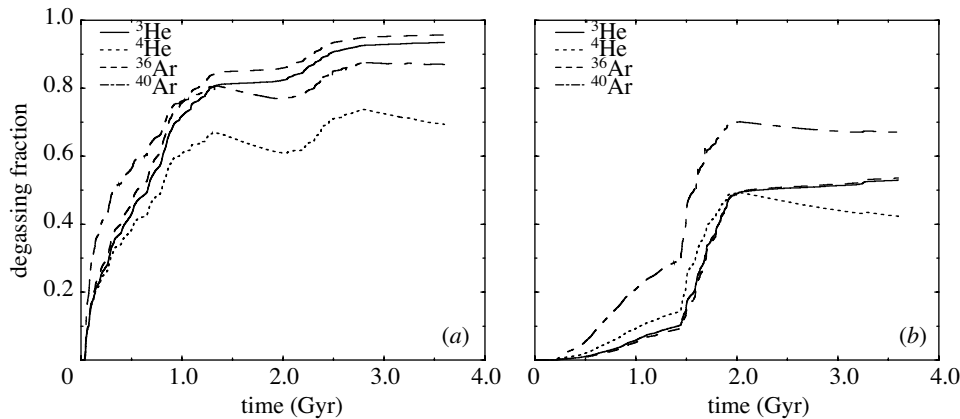
Figure 1. Outgassing of He and Ar isotopes versus time, expressed as a fraction of the total amount of each isotope (which increases with time for ^{4}He and ^{40}Ar): (*a*) case H, (*b*) case L.

thus worth examining. Regarding convective vigour, at the end of the simulations ('present day') the surface heat flux is *ca.* 30 mW m^{-2}, while the root-mean-squared surface velocity is *ca.* 0.3 cm yr^{-1}, values that are factors of approximately 2.6 and 10 lower than Earth's, respectively, implying that the effective Rayleigh number is *ca.* 1.5 orders of magnitude too low.

Regarding viscosity, it is much less temperature dependent than the Earth's, which means that the mantle temperature changes by greater amounts to accommodate changes in the internal heating rate (by self-regulation (Tozer 1972)). In addition, the model viscosity is too high, as indicated by the too-low surface velocities. As a result, the mantle temperature is unrealistically hot in these calculations, resulting in greater amounts of melting and differentiation than is realistic for the Earth. Although several physical properties and parameters affect mantle temperatures in convection calculations (e.g. Tackley 1996*a*), viscosity varies much more than anything else and is likely to be dominant in determining mantle temperature in the Earth.

(*b*) *Outgassing and time evolution*

The time history of outgassing of noble gases (figure 1) indicates that case H is 87% outgassed in radiogenic ^{40}Ar, while case L is 67% outgassed, which, when compared with the geochemically preferred value of 50% (Allègre *et al.* 1996), suggests that these models are more differentiated than the Earth, although outgassing would be greatly reduced if some of the gases were retained in the crust. This is because the model mantle is hotter than realistic, as explained above, which more than compensates for the fact that plate velocities are much lower in the model than in the Earth.

The time history of outgassing for case H (figure 1*a*) indicates an early phase of abundant magmatism and outgassing, followed by a slower phase persisting to the present day. This deceleration is caused by the secular decay of heat-producing elements and by the differentiation and resulting chemical stratification of the mantle as discussed below. In case L, the mantle takes longer to heat up because heat-producing elements are concentrated in a deep layer. This results in an early epoch
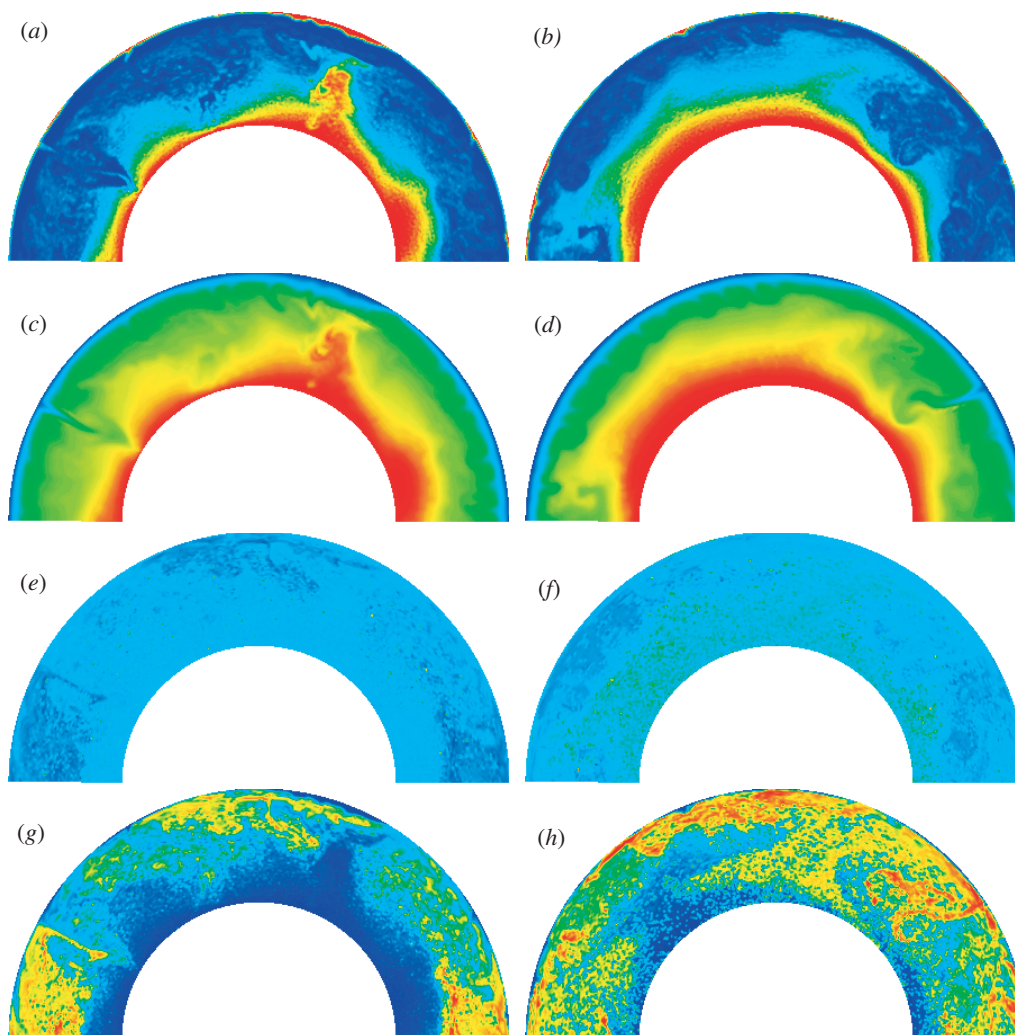
Figure 2. Internal structures after 3.6 Gyr of case H (left column) and case L (right column). (a), (b) Composition, ranging from basalt/eclogite (red) to harzburgite (blue). (c), (d) Temperature field, from 300 K (blue) to 3600 K (red). ^{207}Pb/^{204}Pb for (e) case H, ranging from 14.3 (blue) to 18 (red), and (f) case L, ranging from 14.4 (blue) to 16.6 (red). ^{3}He/^{4}He (relative to atmospheric) for: (g) case H, ranging from 0 (blue) to 54 (red) and (h) case L, ranging from 0 (blue) to 43 (red).

of rigid-lid behaviour and limited magmatism. If a sufficiently lower lithospheric yield stress were assumed, this early rigid lid would not form.

(c) *Interior structure*

(i) *Homogeneous start*

For case H, the compositional field (figure 2a) indicates that a thick layer of dense, subducted oceanic crust has built up at the base of the mantle, with a thin crust near the surface. A compositional gradation exists between these layers, with approx-

imately the upper two-thirds of the mantle being strongly depleted, because residuum from melting is assumed to be buoyant at all depths. Other simulations indicate that the extent of compositional stratification that builds up is strongly dependent on the compositional density contrast.

The dense, recycled layer is enriched in the heat-producing incompatible elements ^{40}K, U and Th because they partition into the crust on melting. The resulting intense heat production causes the layer to become almost as hot as the CMB, as seen in the temperature field (figure 2c). CMB heat flow is low, at 11% of the total heat flow. Upwellings (e.g. plumes) from this layer are suppressed because of the stable compositional gradient that exists in the mantle.

The ^{207}Pb/^{204}Pb ratio (figure 2e) is high in this recycled crustal material, because of the high concentration of U, which produces ^{207}Pb. These ratios are analysed further later. The ^{3}He/^{4}He ratio (figure 2g) is very low in the recycled crustal layer because it is enriched in U and Th, which produce ^{4}He; this dominates any He that was there previously because 99% of the pre-existing He in this material was lost to the atmosphere when the magma erupted. The ^{3}He/^{4}He ratio is high in recycled residuum, however, because it is assumed, based on Hiyagon & Ozima (1986) and Hofmann (1988), that He is less incompatible than U and Th (table 1). Therefore, while almost all of the U and Th are lost during melting, significant amounts of He are retained in the residuum. Lack of U and Th means that the He-isotope ratio is frozen at its (higher than present-day) value. While this is generally consistent with the models of Coltice & Ricard (1999) and Ferrachat & Ricard (2001), they obtained high ^{3}He/^{4}He even when the partition coefficient for He was lower than that for U and Th, because the background mantle became progressively degassed, so its ^{3}He/^{4}He ratio fell faster than that of ancient residuum. This high-^{3}He/^{4}He-ratio material is preferentially located in the upper mantle, directly underneath the lithosphere, because the residuum is buoyant and hence 'floats' to the top. However, because the degree of melting is higher in this model than in the Earth (as discussed earlier), the degree of depletion, and hence the buoyancy of the residuum, may be overestimated.

(ii) *Layered start*

The fields for case L show similar types of structure to those of case H, which may be surprising given the difference in initial conditions. In particular, the dense basal layer is expected to exhibit a high ^{3}He/^{4}He ratio because of the high concentration of ^{3}He that was initially present in the layer. Early in the calculation this was indeed the case: the subducted crust added to the original layer, and the high concentration of U and Th in the recycled crust, produced enough ^{4}He to overwhelm the pre-existing ^{3}He. For this to be prevented, the original layer must have a substantially higher density than subducted crust, and/or a higher initial concentration of ^{3}He.

(d) *Isotope ratios*

Lead–lead isotope diagrams for the two cases (figure 3a,b) show a scatter that lies roughly along the observed MORB–HIMU trend, but extends to even lower and higher values. The average isotope ratios of erupted magmas in the final part of each run (indicated by the vertical line) lie within the observed range of MORB values. The 'ages' that are derived from the slope of the lead–lead diagram are 2.8 and
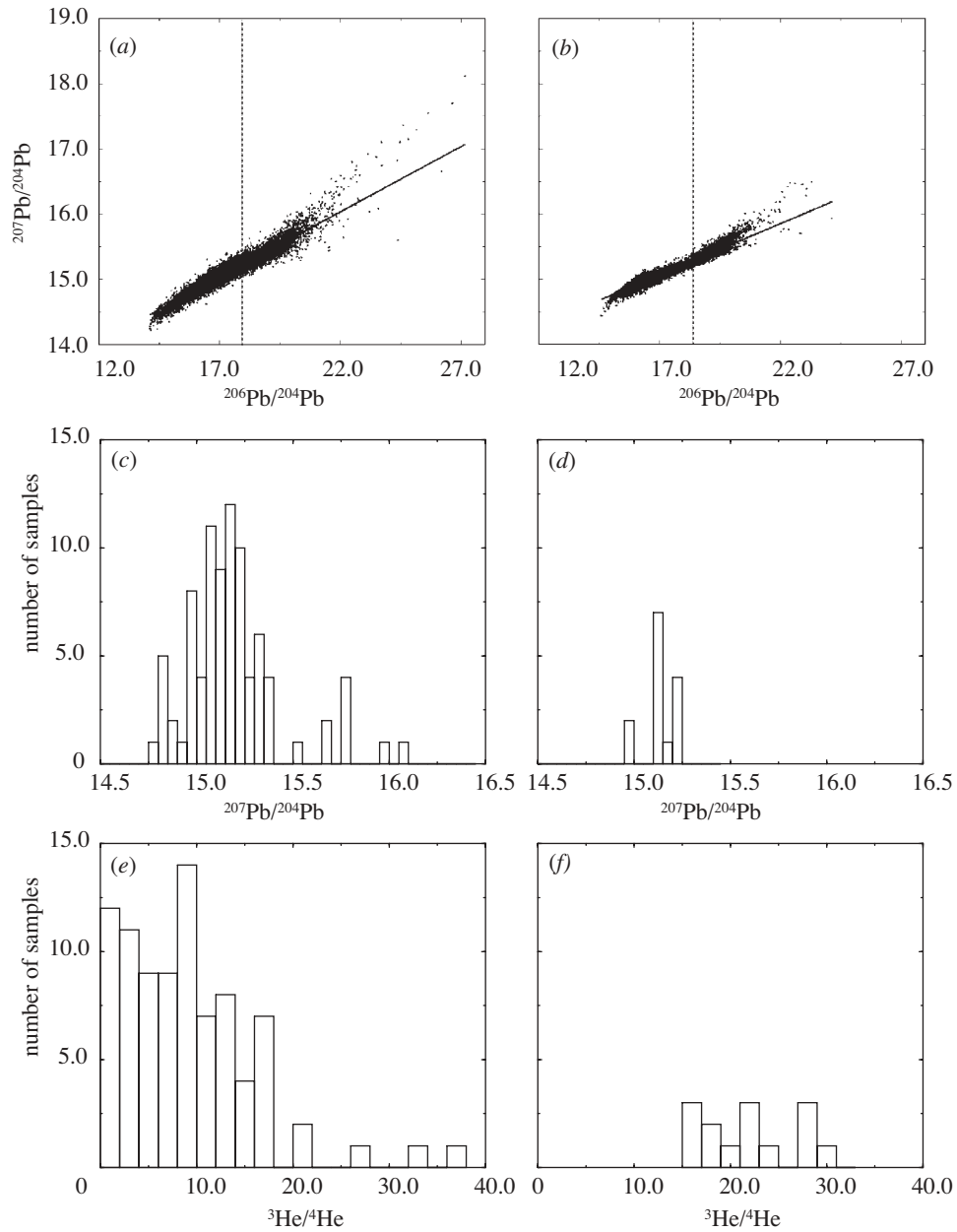
P. J. Tackley and S. Xie

Figure 3. Isotopic information for case H (left column) and for case L (right column).
(*a*), (*b*) Pb–Pb-isotope diagrams for the whole domain, with the vertical line indicating the average composition of erupted magmas and the sloping line being a least-squares fit of the points giving 'ages' of 2.8 and 2.4 Gyr respectively. Histograms show isotope ratios of material that melts in the last 150 Myr of the calculations (case H exhibits more melting than case L during this time period): (*c*), (*d*) ^{207}Pb/^{204}Pb; (*e*), (*f*) ^{3}He/^{4}He relative to atmospheric.

2.4 Gyr, somewhat larger than the 1–2 Gyr obtained for the Earth (Hofmann 1997). The interpretation of this 'age' is complicated for Earth (Albarède 2001; Hofmann 1997); for a simple recycling model such as the present one and that of Christensen & Hofmann (1994), it is related to (although not equal to) the residence time of heterogeneities in the basal layer and would decrease if the subducted crust were less dense than is assumed here.

Since, in reality, isotope ratios can only be measured in erupted material, model isotope ratios for material erupted during the final 150 Myr of each case are presented. The ^{207}Pb/^{204}Pb ratio distribution (figure 3c, d) reflects that obtained in the interior (figure 3a, b). For case H, helium ratios (figure 3e) are distributed around that observed for MORB (approximately eight times atmospheric), with a few high values of up to 37 times atmospheric, compatible with some hotspots on Earth. For case L, however, He-ratio values are clustered around an intermediately high value of 20 times atmospheric and seem to be dominated by high-^{3}He/^{4}He buoyant residuum material that exists under the lithosphere.

6. Conclusions

While geochemistry indicates the need for several reservoirs, geophysical observations constrain the plausible location of mantle reservoirs to be a thin (D'') layer, isolated pockets or piles, probably under large-scale mantle upwellings, or distributed through the mantle as high-viscosity 'plums'/'blobs' or thin strips. Numerical convection codes with integrated geochemical tracking are emerging as a powerful tool for testing hypothesized models of the mantle. Preliminary simulations presented here are more highly differentiated than Earth but display some of the proposed thermochemical processes, including generation of a HIMU reservoir by recycling of crust and generation of a high-^{3}He/^{4}He reservoir by recycling of residuum. The resulting high-^{3}He/^{4}He material tends to aggregate in the upper mantle, so would be expected to be sampled in MORB melting. If primitive material exists as a dense basal layer, it must be even more dense than subducted crustal material in order not to mix and have its primitive (high-^{3}He) signature overwhelmed. However, since the model is far from Earth like, these findings are only tentative.

The existing model needs to be made more Earth like in terms of rheology, convective vigour and amount of differentiation (i.e. amount of melting). Greater convective vigour will also result in faster mixing, which is important in rehomogenizing the differentiated components. Such realism should be possible in two dimensions in the near future.

Several other model shortcomings need to be addressed, perhaps most acutely the lack of continents, which are thought to play a major role in the Earth's chemical differentiation. A better model of density as a function of composition and pressure (and temperature) is required (e.g. Ringwood 1990), although there is considerable uncertainty about the correct values particularly in deep mantle where eclogite may even be less dense than pyrolite (Kesson *et al.* 1998; Ono *et al.* 2001). Melting and differentiation is treated using a crude parametrization of a complex physical process that is still not well understood. The initial condition is not known. Thus, better data on the dependence of density on composition in the deep mantle, 'effective' partition coefficients, etc., are keenly needed.

References

Albarède, F. 1998 Time-dependent models of U–Th–He and K–Ar evolution and the layering of mantle convection. *Chem. Geol.* **145**, 413–429.

Albarède, F. 2001 Radiogenic ingrowth in systems with multiple reservoirs: applications to the differentiation of the mantle–crust system. *Earth Planet. Sci. Lett.* **189**, 59–73.

Allègre, C. J. & Turcotte, D. L. 1986 Implications of a 2-component marble-cake mantle. *Nature* **323**, 123–127.

Allègre, C. J., Hofmann, A. & O'Nions, K. 1996 The argon constraints on mantle structure. *Geophys. Res. Lett.* **23**, 3555–3557.

Becker, T. W., Kellogg, J. B. & O'Connell, R. J. 1999 Thermal constraints on the survival of primitive blobs in the lower mantle. *Earth Planet. Sci. Lett.* **171**, 351–365.

Brunet, D. & Machetel, P. 1998 Large-scale tectonic features induced by mantle avalanches with phase, temperature, and pressure lateral variations of viscosity. *J. Geophys. Res.* **103**, 4929–4945.

Butler, S. & Peltier, W. R. 1997 Internal thermal-boundary-layer stability in phase-transition modulated convection. *J. Geophys. Res.* **102**, 2731–2749.

Castillo, P. 1988 The Dupal anomaly as a trace of the upwelling lower mantle. *Nature* **336**, 667–670.

Chopelas, A. & Boehler, R. 1992 Thermal expansivity in the lower mantle. *Geophys. Res. Lett.* **19**, 1983–1986.

Christensen, U. 1989 Mixing by time-dependent convection. *Earth Planet. Sci. Lett.* **95**, 382–394.

Christensen, U. R. 1996 The influence of trench migration on slab penetration into the lower mantle. *Earth Planet. Sci. Lett.* **140**, 27–39.

Christensen, U. R. & Hofmann, A. W. 1994 Segregation of subducted oceanic crust in the convecting mantle. *J. Geophys. Res.* **99**, 19 867–19 884.

Coltice, N. & Ricard, Y. 1999 Geochemical observations and one layer mantle convection. *Earth Planet. Sci. Lett.* **174**, 125–137.

Coltice, N., Ferrachat, S. & Ricard, Y. 2000 Box modeling the chemical evolution of geophysical systems: case study of the Earth's mantle. *Geophys. Res. Lett.* **27**, 1579–1582.

Davies, G. F. 1984 Geophysical and isotopic constraints on mantle convection—an interim synthesis. *J. Geophys. Res.* **89**, 6017–6040.

Davies, G. F. 1999 Geophysically constrained mantle mass flows and the ^{40}Ar budget: a degassed lower mantle? *Earth Planet. Sci. Lett.* **166**, 149–162.

Ferrachat, S. & Ricard, Y. 1998 Regular vs. chaotic mantle mixing. *Earth Planet. Sci. Lett.* **155**, 75–86.

Ferrachat, S. & Ricard, Y. 2001 Mixing properties in the Earth's mantle: effects of the viscosity stratification and of oceanic crust segregation. *Geochem. Geophys. Geosyst.* **2**, 2000GC000092.

Gable, C. W., O'Connell, R. J. & Travis, B. J. 1991 Convection in three dimensions with surface plates: generation of toroidal flow. *J. Geophys. Res.* **96**, 8391–8405.

Graham, D., Lupton, J., Albarède, F. & Condomines, M. 1990 Extreme temporal homogeneity of helium isotopes at Piton de la Fournaise, Réunion Island. *Nature* **347**, 545–548.

Grand, S. P., van der Hilst, R. D. & Widiyantoro, S. 1997 Global seismic tomography: a snapshot of convection in the Earth. *GSA Today* **7**, 1–7.

Gurnis, M. & Davies, G. F. 1986 The effect of depth-dependent viscosity on convective mixing in the mantle and the possible survival of primitive mantle. *Geophys. Res. Lett.* **13**, 541–544.

Gurnis, M., Mitrovica, J. X., Ritsema, J. & van Heijst, H.-J. 2000 Constraining mantle density structure using geological evidence of surface uplift rates: the case of the African Superplume. *Geochem. Geophys. Geosyst.* **1**, 1999GC000035.

Hart, S. R., 1984 A large-scale anomaly in the southern hemisphere mantle. *Nature* **309**, 753–757.

Herzberg, C., Raterron, P. & Zhang, J. 2000 New experimental observations on the anhydrous solidus for peridotite klb-1. *Geochem. Geophys. Geosyst.* **1**, 2000GC000089.

Hiyagon, H. & Ozima, M. 1986 Partition of noble gases between olivine and basalt melt. *Geochim. Cosmochim. Acta* **50**, 2045–2057.

Hofmann, A. W. 1988 Chemical differentiation of the Earth: the relationship between mantle, continental crust, and oceanic crust. *Earth Planet. Sci. Lett.* **90**, 297–314.

Hofmann, A. W. 1997 Mantle geochemistry: the message from oceanic volcanism. *Nature* **385**, 219–229.

Hofmeister, A. M. 1999 Mantle values of thermal conductivity and the geotherm from phonon lifetimes. *Science* **283**, 1699–1706.

Ishii, M. & Tromp, J. 1999 Normal-mode and free-air gravity constraints on lateral variations in velocity and density of Earth's mantle. *Science* **285**, 1231–1235.

Jeanloz, R. & Lay, T. 1993 The core–mantle boundary. *Scient. Am.* **268**, 48–55.

Karato, S. & Wu, P. 1993 Rheology of the upper mantle: a synthesis. *Science* **260**, 771–778.

Kellogg, L. H. & Turcotte, D. L. 1990 Mixing and the distribution of heterogeneities in a chaotically convecting mantle. *J. Geophys. Res.* **95**, 421–432.

Kellogg, L. H., Hager, B. H. & van der Hilst, R. D. 1999 Compositional stratification in the deep mantle. *Science* **283**, 1881–1884.

Kesson, S. E., Gerald, J. D. F. & Shelley, J. M. 1998 Mineralogy and dynamics of a pyrolite lower mantle. *Nature* **393**, 252–255.

Lay, T. & Helmberger, D. V. 1983 A shear velocity discontinuity in the lower mantle. *Geophys. Res. Lett.* **10**, 63–66.

Lay, T., Williams, Q. & Garnero, E. J. 1998 The core–mantle boundary layer and deep Earth dynamics. *Nature* **392**, 461–468.

McNamara, A. K. & van Keken, P. E. 2000 Cooling of the Earth: a parameterized convection study of whole versus layered models. *Geochem. Geophys. Geosyst.* **1**, 2000GC000045.

Manga, M. 1996 Mixing of heterogeneities in the mantle: effect of viscosity differences. *Geophys. Res. Lett.* **23**, 403–406.

Masters, G., Laske, G., Bolton, H. & Dziewonski, A. 2000 The relative behavior of shear velocity, bulk sound speed, and compressional velocity in the mantle: implications for chemical and thermal structure. In *Mineral physics and seismic tomography* (ed. S. E. A. Karato). Washington, DC: American Geophysical Union.

Montague, N. L., Kellogg, L. H. & Manga, M. 1998 High Rayleigh number thermo-chemical models of a dense boundary layer in D''. *Geophys. Res. Lett.* **25**, 2345–2348.

Moresi, L. & Solomatov, V. 1998 Mantle convection with a brittle lithosphere: thoughts on the global tectonic styles of the Earth and Venus. *Geophys. J. Int.* **133**, 669–682.

Olson, P. & Kincaid, C. 1991 Experiments on the interaction of thermal convection and compositional layering at the base of the mantle. *J. Geophys. Res.* **96**, 4347–4354.

Ono, S., Ito, E. & Katsura, T. 2001 Mineralogy of subducted basaltic crust (MORB) from 25 to 37 GPa, and chemical heterogeneity of the lower mantle. *Earth Planet. Sci. Lett.* **190**, 57–63.

Phipps Morgan, J. & Morgan, J. 1999 Two-stage melting and the geochemical evolution of the mantle: a recipe for mantle plum-pudding. *Earth Planet. Sci. Lett.* **170**, 215–239.

Ringwood, A. E. 1990 Slab–mantle interactions. 3. Petrogenesis of intraplate magmas and structure of the upper mantle. *Chem. Geol.* **82**, 187–207.

Ritsema, J., Ni, S., Helmberger, D. V. & Crotwell, H. P. 1998 Evidence for strong shear velocity reductions and velocity gradients in the lower mantle beneath Africa. *Geophys. Res. Lett.* **25**, 4245–4248.

Schmalzl, J. & Hansen, U. 1994 Mixing the Earth's mantle by thermal-convection: a scale-dependent phenomenon. *Geophys. Res. Lett.* **21**, 987–990.

Schmalzl, J., Houseman, G. A. & Hansen, U. 1995 Mixing properties of three-dimensional (3D) stationary convection. *Phys. Fluids* **7**, 1027–1033.

Schmalzl, J., Houseman, G. A. & Hansen, U. 1996 Mixing in vigorous, time-dependent three-dimensional convection and application to Earth's mantle. *J. Geophys. Res.* **101**, 21 847–21 858.

Sidorin, I., Gurnis, M. & Helmberger, D. V. 1999 Dynamics of a phase change at the base of the mantle consistent with seismological observations. *J. Geophys. Res.* **104**, 15 005–15 024.

Stacey, F. D. 1992 Physics of the Earth, 3rd ed. Kenmore, Australia: Brookfield Press.

Tackley, P. J. 1993 Effects of strongly temperature-dependent viscosity on time-dependent, three-dimensional models of mantle convection. *Geophys. Res. Lett.* **20**, 2187–2190.

Tackley, P. J. 1996*a* Effects of strongly variable viscosity on three-dimensional compressible convection in planetary mantles. *J. Geophys. Res.* **101**, 3311–3332.

Tackley, P. J. 1996*b* On the ability of phase transitions and viscosity layering to induce long-wavelength heterogeneity in the mantle. *Geophys. Res. Lett.* **23**, 1985–1988.

Tackley, P. J. 1998 Three-dimensional simulations of mantle convection with a thermochemical CMB boundary layer: D''? In *The core–mantle boundary region* (ed. M. Gurnis, M. E. Wysession, E. Knittle & B. A. Buffett), vol. 28, pp. 231–253. Washington, DC: American Geophysical Union.

Tackley, P. J. 2000*a* Mantle convection and plate tectonics: towards an integrated physical and chemical theory. *Science* **288**, 2002.

Tackley, P. J. 2000*b* Self-consistent generation of tectonic plates in time-dependent, three-dimensional mantle convection simulations. Part 1. Pseudo-plastic yielding. *Geochem. Geophys. Geosyst.* **1**, 2000GC000036.

Tackley, P. J. 2000*c* Self-consistent generation of tectonic plates in time-dependent, three-dimensional mantle convection simulations. Part 2. Strain weakening and asthenosphere. *Geochem. Geophys. Geosyst.* **1**, 2000GC000043.

Tackley, P. J. 2002 Strong heterogeneity caused by deep mantle layering. *Geochem. Geophys. Geosystems* **3**, 2001GC000167.

Tackley, P. J., Stevenson, D. J., Glatzmaier, G. A. & Schubert, G. 1994 Effects of multiple phase transitions in a three-dimensional spherical model of convection in Earth's mantle. *J. Geophys. Res.* **99**, 15 877–15 901.

Ten, A. A., Podladchikov, Y. Y., Yuen, D. A., Larsen, T. B. & Malevsky, A. V. 1998 Comparison of mixing properties in convection with the particle-line method. *Geophys. Res. Lett.* **25**, 3205–3208.

Tozer, D. C. 1972 The present thermal state of the terrestrial planets. *Phys. Earth Planet. Inter.* **6**, 182–197.

Turcotte, D. L. 1993 An episodic hypothesis for Venusian tectonics. *J. Geophys. Res.* **98**, 17 061–17 068.

van Keken, P. E. & Ballentine, C. J. 1998 Whole-mantle versus layered mantle convection and the role of a high-viscosity lower mantle in terrestrial volatile evolution. *Earth Planet. Sci. Lett.* **156**, 19–32.

van Keken, P. E. & Ballentine, C. J. 1999 Dynamical models of mantle volatile evolution and the role of phase transitions and temperature-dependent rheology. *J. Geophys. Res.* **104**, 7137–7151.

van der Hilst, R. D., Widlyantoro, S. & Engdahl, E. R. 1997 Evidence for deep mantle circulation from global tomography. *Nature* **386**, 578–584.

Vidale, J. E., Schubert, G. & Earle, P. S. 2001 Unsuccessful initial search for a midmantle chemical boundary layer with seismic arrays. *Geophys. Res. Lett.* **28**, 859–862.

Weinstein, S. A. 1992 Induced compositional layering in a convecting fluid layer by an endothermic phase-transition. *Earth Planet. Sci. Lett.* **113**, 23–39.

Zerr, A., Diegeler, A. & Boehler, R. 1998 Solidus of Earth's deep mantle. *Science* **281**, 243–246.